

Caisson foundation subjected to normal faulting: Experiment vs. analysis

I. Anastasopoulos¹

National Technical University, Athens, Greece

M. Loli

National Technical University, Athens, Greece

F. Bransby

University of Dundee, UK

G. Gazetas

National Technical University, Athens, Greece

ABSTRACT

Dramatic failures have occurred in large magnitude earthquakes due to the interplay of surface structures with outcropping fault ruptures. Employing both centrifuge testing and numerical analysis, this paper explores the mechanisms of normal fault rupture interaction with rigid caisson foundations. First, a series of centrifuge tests were conducted to study the response of a 5m x 5m x 10 m caisson founded on a layer of dry dense sand. Nonlinear 3-D numerical modelling of the problem was then developed and adequately validated against the centrifuge tests results. Depending on its position relative to the fault, the caisson is found to interact with the fault rupture, sometimes modifying spectacularly the free field rupture path. Acting as a kinematic constraint, the caisson causes the rupture to divert on either one, or both, of its sides. The numerical study was subsequently extended to a parametric investigation of the effect of the exact position of the caisson relative to the fault outcrop. Different mechanisms taking place for different caisson positions are identified, and their effect on the response of the soil–foundation system is discussed.

RÉSUMÉ

Employant des tests centrifugeuse et l'analyse numérique, ce document explore les mécanismes d'interaction d'une rupture normale avec des fondations caisson rigide. Une série de tests centrifugeuse ont été menées pour étudier la performance d'un caisson fondée sur une couche de sable dense. Modélisation numérique du problème a ensuite été développée et validée contre les tests centrifugeuse. Selon sa position par rapport à la faute, le caisson se trouve à interagir avec la rupture. Agissant comme une contrainte cinématique, le caisson provoque la rupture de dévier sur l'un ou les deux, de ses côtés. L'étude numérique a ensuite été étendue à une enquête paramétrique de l'effet de la position exacte du caisson par rapport à la faute. Différents mécanismes sont identifiés pour les positions différentes du caisson, et leur effet sur la réponse du système sol-fondation est discuté.

Keywords: Fault Rupture; Centrifuge Modelling; Numerical Modelling; Soil–Structure Interaction.

1 INTRODUCTION

Several studies have considered the response of a structural system interacting with a propagating fault rupture, revealing that the presence of a structure may alter, sometimes dramatically, the free field rupture path. The mechanics of this

phenomenon, termed Fault Rupture–Soil–Foundation–Structure Interaction (FR–SFSI), have been analyzed on the basis of : interpretation of real case histories [1] ; centrifuge experiments [2] ; and numerical analyses [3-5].

Aiming to extend the research work on the mechanisms of FR–SFSI, which has been so far

¹ Corresponding Author.

(more or less) limited to the response of shallow foundations, this paper investigates the interaction of deep embedded foundations (caissons) with a rupturing normal fault. A combination of centrifuge model testing and numerical simulation of the problem was employed to this end. A series of centrifuge experiments were carried out to investigate the response of the caisson foundation, concentrating on the effects of its position relative to the fault rupture. After validating the effectiveness of the numerical analysis methodology against experimental results, a parametric study was conducted to offer additional insight into the effect of foundation location and these results are discussed with respect to future bridge pier design.

2 METHODOLOGY

Figure 1 illustrates schematically the main features of the studied problem and defines the Cartesian coordinate system adopted. A 5 x 5 x 10 (m) square in plan caisson foundation is considered, supported on a 15 m thick layer of dense ($D_r \approx 80\%$) dry sand. It carries a total vertical load of approximately 20 MN, which represents the weight of a superstructure of significant size (e.g., a medium span bridge). Normal (i.e. downwards) fault displacement of vertical amplitude h (throw) is applied at the bedrock. The displaced block of soil (i.e. the hanging wall) moves downwards with a dip angle of 60° , whereas the footwall remains stationary. The fault deformation forces the caisson to move as a rigid body, experiencing both translational δ and rotational θ displacements.

The location of the caisson relative to the outcropping fault rupture is expressed through parameter s , which is defined as the distance between the caisson right corner and the point that the free-field (unperturbed) fault rupture would cross the foundation base (Figure 2). In other words, s indicates the point that the fault rupture would interact with the caisson if fault rupture–caisson interaction did not take place to alter the rupture path. In the following presentation of results s is normalized by the foundation width B .

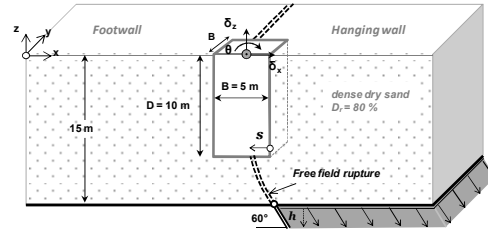


Figure 1. Schematic of the studied problem indicating the basic parameters and dimensions at prototype scale.

2.1 Centrifuge Modelling

A series of centrifuge model tests were conducted in the beam centrifuge of the University of Dundee at an operational acceleration of $100g$ ($N = 100$). The experimental study aimed at investigating the mechanisms of fault rupture–caisson interaction with regard to the caisson position relative to the fault (s). Hence, three centrifuge tests were conducted (ML-07, ML-08 and ML-10), where the caisson was placed at three different positions, as indicated in Table 1, together with one free field test (Test ML-06).

Figure 2 displays the physical model within the strongbox indicating the faulting apparatus. The 150 mm deep (i.e. 15 m at prototype scale) soil layer was prepared by dry air pluviation of Fontainebleau sand. The sand was pluviated from a specific height with a fixed sieve aperture to control the mass flow rate, giving a uniform density $D_r \approx 80\%$ ($\gamma = 16.11 \text{ kN/m}^3$). Direct shear tests were conducted to investigate the soil stress–strain and volumetric behaviour. For a mean value of relative soil density $D_r = 80\%$, the peak and residual friction angles of the soil were measured as $\phi_{peak} = 37^\circ$ and $\phi_{res} = 31^\circ$ at a normal effective stress representative of the middle of the soil depth (i.e. $\sigma'_v = 120 \text{ kPa}$ for depth $z = -7.5 \text{ m}$). The dilation angle ψ was measured as approximately 10° for the same representative normal stress.

Table 1. Centrifuge testing programme.

Test ID	Caisson Position [s/B]	Soil Density [Dr (%)]
ML-06	–	77.5
ML-07	0.78	70.0
ML-08	0.28	74.6
ML-10	0.58	76.0

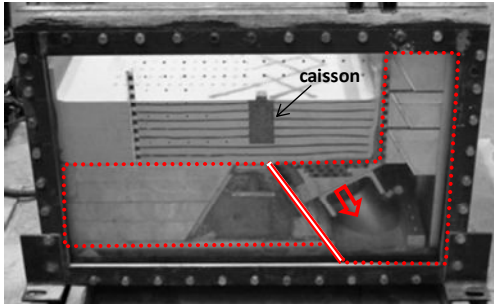


Figure 2. Photo of the model and the fault rupture apparatus used in centrifuge testing.

The caisson model was made of steel, having a total mass of 1.025 kg (corresponding to a prototype of 2050 Mg). Aiming to have realistically rough soil–caisson interfaces, the caisson model sides were needle-gunned (except the side that faced the Perspex window of the strongbox). The frictional properties at the caisson–soil interface were measured through direct-shear tests performed on similar needle-gunned steel specimens, which gave a friction angle of 19.8° at peak and 17° at residual conditions. It should be noted that the Perspex acts as a plane of symmetry, and hence the caisson dimensions perpendicular to the Perspex face were half the prototype values.

2.2 Numerical Modelling

Numerical simulations of the centrifuge model tests were performed employing the finite element (FE) method, using the ABAQUS code. The model dimensions were chosen to be the same as the dimensions of the physical model at prototype scale. Figure 3 shows the geometry, the boundary conditions and the main features of the FE mesh. Mesh discretization was deter-

mined through a sensitivity analysis so as to provide adequate accuracy and time efficiency.

Soil modelling was based on the methodology of Anastasopoulos et al [4]. An elasto-plastic constitutive relationship was used and encoded in ABAQUS through a user subroutine. This assumes elastic pre-yield soil behaviour defined by the secant shear modulus G_s , which was increased linearly with soil depth. Failure was defined by the Mohr–Coulomb criterion accompanied with an isotropic strain softening law which degrades the friction (ϕ) and dilation (ψ) angles linearly with octahedral plastic shear strain.

Calibration of the soil model parameters was performed with respect to the results of direct shear tests taking into account the scale effects associated with shear-band modelling.

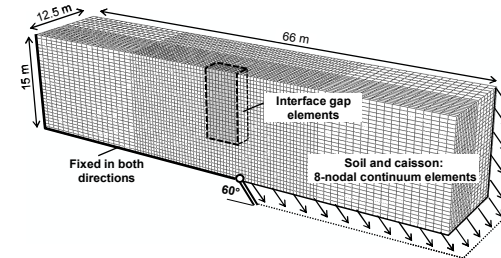


Figure 3. Photo of the model and the fault rupture apparatus used in centrifuge testing.

3 PRESENTATION OF CHARACTERISTIC RESULTS

For the sake of brevity, results are herein presented in detail only for one characteristic fault rupture–caisson interaction test, namely that wherein the caisson was positioned at a relative distance $s/B = 0.28$ from the fault (ML_08). Yet, all the tests of Table 1 have been comprehensively reported in [6].

Figure 4a displays a set of the centrifuge model test images, captured at different levels of fault displacement h , and demonstrates a progressive type of failure associated with the interplay between different failure mechanisms. First, for $h = 0.6$ m, the caisson acting as a kinematic constraint forces the rupture to deviate signifi-

cantly from its free field path, actually changing orientation, and to propagate towards the hanging-wall (right) caisson edge.

Shear stresses develop along the right sidewall of the caisson and its consequent clockwise rotation causes active type stress conditions to take place on the other (left, footwall) side of the caisson. An active failure wedge forms on the footwall side of the foundation for $h = 1.0$ m, clearly indicated by the respective shear strain contours in Figure 4b. Soil failure on this side, as well as the soil distress underneath the foundation base due to its significant rotation, “facilitate” the diversion of the rupture to the left of the caisson and a secondary rupture plane (F2) is mobilized.

Thereafter, a rather subtle interaction mechanism is observed, involving the formation of active and passive failure wedges on the left(footwall) and right (hanging-wall) side of the caisson respectively, and fault propagation on both sides concurrently (see image for $h = 2.0$ m and the equivalent shear strain contours).

The numerically computed shear strain contours shown in Figure 4c indicate that the numerical analysis captures the previously described fault rupture–caisson interaction mechanisms closely, demonstrating excellent agreement with the experiment.

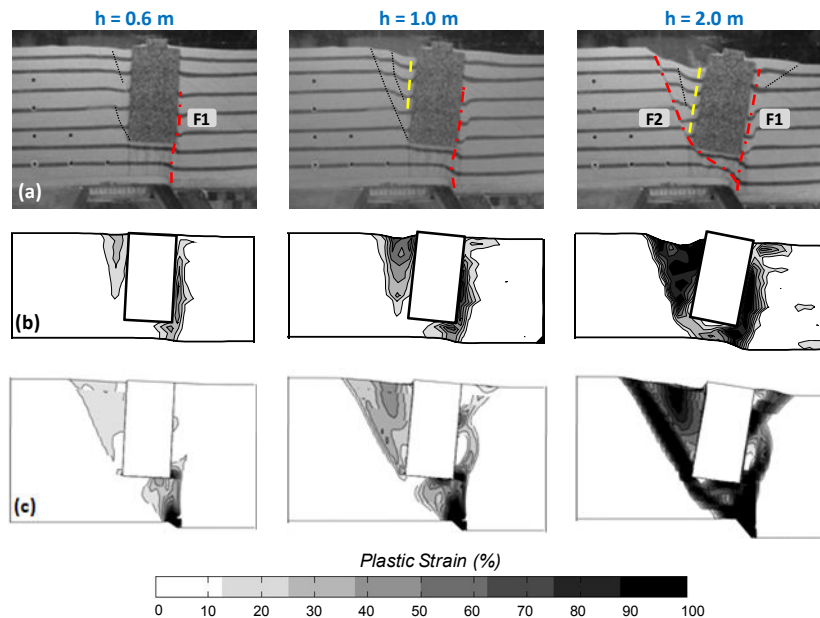


Figure 4. Normal Fault rupture–caisson interaction at different stages of faulting for $s/B = 0.28$ (Test ML_08): (a) centrifuge test model images; (b) contours of shear strains developed within the soil in the centrifuge test compared to (c) the corresponding numerical analysis.

Regarding foundation performance, the extensive soil failure around the caisson provoked significant displacements in both the presented tests (Figure 5). The figure also indicates the very sat-

isfactory agreement between analysis and experiment throughout the whole range of the examined fault displacements and for both types of tectonic movement.

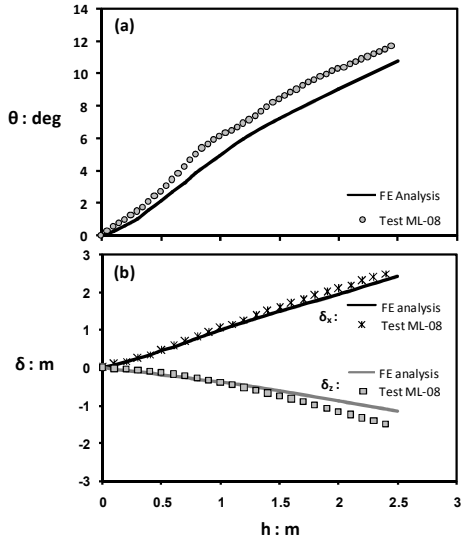


Figure 5. Response of the caisson versus the applied fault displacement for $s/B = 0.28$ (test ML-08) and comparison with the numerical analysis in terms of: (a) caisson rotation; and (b) horizontal and vertical displacements.

It should be noted that in this particularly destructive case of normal faulting at $s/B = 0.28$, the rotation of the caisson, reaching about 12° for $h = 2.5$, exceeded by a factor of more than two the rotation experienced in the other two normal fault tests. This indicated the determinative role of the exact caisson position on the prevailing interaction mechanisms and the subsequent caisson response and motivated the following parametric investigation of the effect of parameter s .

4 PARAMETRIC INVESTIGATION OF THE EXACT CAISSON POSITION

Figure 6 summarizes the results with respect to foundation performance for different levels of fault throw h as calculated from a series of FE analyses. The different failure mechanisms taking place are also indicated by the shear strain finite element contours that correspond to different points (positions) in the graph. Three different interaction mechanisms can be identified, dividing the graph in three zones (A, B, and C).

Mechanism A ($s/B < -0.4$; i.e. $s < -2$ m) takes place when the fault rupture "grazes" the hanging-wall (right) sidewall of the caisson, missing its base by 2 m or more. The rupture path is refracted on the rigid sidewall and deviated towards the hanging-wall (to the right). The caisson remains on the footwall side of the fault, and experiences limited distress for all levels of fault throw h . This is presumably the most favourable area of possible caisson positions.

Mechanism B ($-0.4 \leq s/B < 0.6$; i.e. $-2 \text{ m} \leq s < 3 \text{ m}$) is prevalent when the fault rupture crosses the caisson body near its right base corner. As discussed previously for test ML-08 ($s/B = 0.28$), the interaction of the caisson with the fault rupture is in this case quite complex, involving: (i) bifurcation of the shear zone along both sides of the caisson, (ii) formation of an active failure wedge at the footwall (left) side of the caisson due to its substantial rotation, and (iii) formation of a passive-type failure wedge at the hanging-wall (right) side of the caisson (also due to the rotation). This is probably the most detrimental position for the response of the system.

Mechanism C ($s/B \geq 0.6$; i.e. $s > 3 \text{ m}$) prevails when the fault rupture crosses the caisson close to its footwall (left) corner, or misses it completely on the footwall (left) side. The rupture is diverted towards the footwall and the caisson translates downwards, following the hanging wall, with only minor rotation.

5 SUMMARY & CONCLUSIONS

This paper has presented a combined experimental and numerical study on the interaction of normal faults with rigid caisson foundations. The key conclusions can be summarized as follows:

- Caisson foundations interact with the fault rupture changing sometimes dramatically its free field path. The rigid caisson body acts as a kinematic constraint, which forces the fault to divert.
- The numerical method was validated through successful comparisons with centrifuge test results, revealing its effectiveness.
- The validation of the numerical method allowed the conduction of a parametric study to further investigate the effect of the exact founda-

tion position, which proved to be a determinative parameter controlling the response of the system.

ACKNOWLEDGEMENTS

NTUA authors would like to acknowledge financial support from the EU 7th Framework research project funded through the European Research Council's Programme "Ideas", Support for Frontier Research – Advanced Grant, under Contract number ERC-2008-AdG 228254-DARE.

REFERENCES

- [1] Anastasopoulos, I. & Gazetas G. (2007). Foundation-Structure Systems over a Rupturing Normal Fault: Part I. Observations after the Kocaeli 1999 Earthquake. *Bulletin of Earthquake Engineering*, 5, No. 3, 253–275.
- [2] Bransby, M.F. Davies, M.C.R. El Nahas, A. & Nagaoka, S. (2008a). Centrifuge modelling of normal fault-foundation interaction. *Bulletin of Earthquake Engineering*, 6, No. 4, 585-605.
- [3] Paolucci, R. & Yilmaz, M.T. (2008). Simplified theoretical approaches to earthquake fault rupture–shallow foundation interaction. *Bulletin of Earthquake Engineering*, 6, No. 4, 629-644.
- [4] Anastasopoulos, I. Gazetas, G. Bransby, M.F. Davies, M.C.R. & El Nahas, A. (2007). Fault Rupture Propagation through Sand : Finite Element Analysis and Validation through Centrifuge Experiments. *Journal of Geotechnical and Geoenvironmental Engineering*, ASCE, 133, No. 8, 943–958.
- [5] Anastasopoulos, I. Gazetas, G. Bransby, M.F. Davies, M.C.R. & El Nahas, A. (2009). Normal Fault Rupture Interaction with Strip Foundations. *Journal of Geotechnical and Geoenvironmental Engineering*, ASCE, 135, No. 3, 359-370.
- [6] Loli, M. Bransby, M.F. Anastasopoulos, I. Gazetas, G. (2010). Interaction of Caisson Foundations with a Seismically Rupturing Normal Fault : Centrifuge Testing versus Numerical Simulation. *Geotechnique*, accepted for publication.

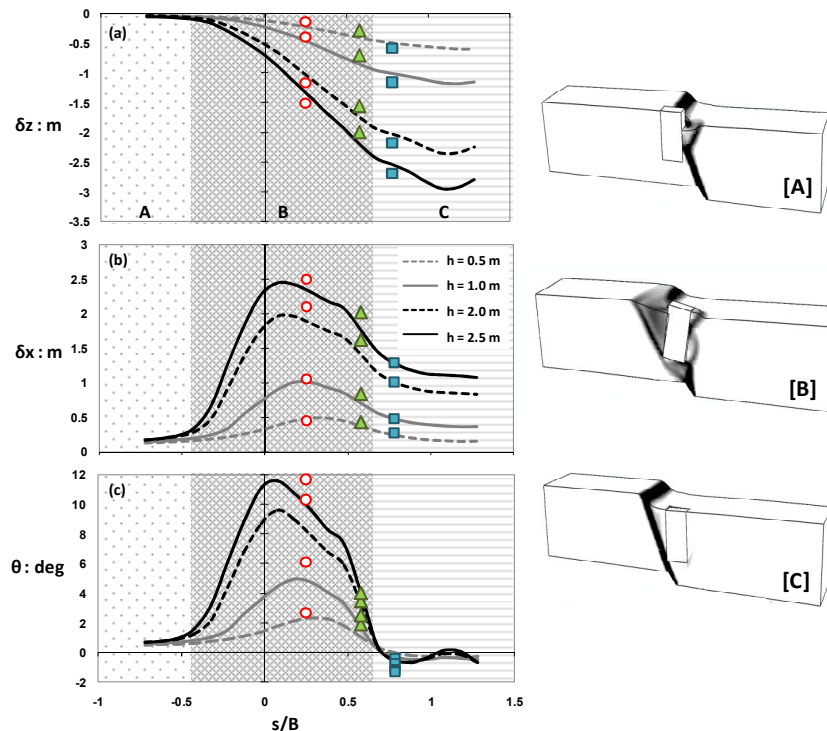


Figure 6. The effect of the exact caisson location (s) on the mechanisms of fault rupture–caisson interaction and the consequent caisson response for the case of reverse tectonic movement: (a) vertical displacements, (b) horizontal displacements, and (c) rotation for different levels of throw.